

Tropical Stationary Waves in a Nonlinear Shallow-Water Model with Realistic Basic States

IAN KRAUCUNAS* AND DENNIS L. HARTMANN

Department of Atmospheric Sciences, University of Washington, Seattle, Washington

(Manuscript received 14 October 2005, in final form 1 August 2006)

ABSTRACT

The nonlinear shallow-water equations are used to study the tropical stationary wave response to steady thermal forcing near the equator in earthlike zonally symmetric basic states. A thin (200 m) fluid layer is superimposed over a large (1500 m) zonally symmetric topography distribution that decreases smoothly from the Tropics to the Poles, thus providing the large meridional height gradients required to maintain realistic zonal-mean zonal winds without introducing unrealistically large tropical wave speeds. A mean meridional circulation is maintained by relaxing the fluid toward its initial, global-mean depth. Both hemispherically symmetric (equinoctial) and hemispherically asymmetric (solstitial) basic states are considered. Stationary waves are generated by adding a fixed mass source/sink distribution near the equator.

The presence of westerly zonal-mean winds in the subtropics amplifies the steady eddy response to the tropical mass forcing and shifts the Rossby gyres poleward and eastward, relative to their position in a resting basic state. When either the mass forcing or the center of the topography distribution is moved off the equator, the eddy response develops considerable hemispheric asymmetry. When the eddy forcing is centered in the “summer” hemisphere of the solstitial basic state, the eddy response exhibits a similar amplitude in both hemispheres, which suggests that the considerable hemispheric symmetry of the observed seasonally varying eddy circulations in the tropical upper troposphere may be attributed to the tendency for the maximum zonal-mean and eddy diabatic heating to occur in the same latitude band throughout the seasonal cycle. Hemispheric asymmetry in either the basic state or the eddy forcing also leads to cross-equatorial eddy momentum fluxes. Experiments performed using a balanced basic state with zero-mean meridional flow indicate that the cross-equatorial mean meridional winds play a significant role in promoting the propagation of wave activity across the equator under solstitial conditions.

1. Introduction

The shallow-water equations are often used to isolate the dynamics of an individual baroclinic mode or a particular isentropic layer in a continuously stratified atmosphere. In this paper, we focus on the stationary waves in the tropical upper troposphere, which can be modeled in the shallow-water framework by choosing a small layer depth and introducing a fixed pattern of mass sources and sinks to represent persistent horizon-

tal variations in diabatic heating at low latitudes. The first papers to employ this technique were Matsuno (1966) and Gill (1980), who examined the linear response on an equatorial beta plane in a resting basic state and interpreted the resulting wave structures in terms of forced Kelvin and Rossby waves. Spherical geometry (Gill 1982), nonlinearity (Van Tuyl 1986; Gill and Phillips 1986), and horizontally uniform zonal winds (Lau and Lim 1982; Lim and Chang 1983; Phillips and Gill 1987) were subsequently found to induce significant changes in the shallow-water response to tropical eddy forcing, including the formation of an extratropical wave train when the mean winds are westerly and the layer depth is sufficiently large. Lau and Lim (1984) extended this analysis by considering the combined effects of spherical geometry, nonlinearity, and realistic mean winds.

Subsequent studies of stationary waves in the upper troposphere have mainly focused on either the extra-

* Current affiliation: Board on Atmospheric Sciences and Climate, National Research Council/The National Academies, Washington, D.C.

Corresponding author address: Dr. Ian Kraucunas, Board on Atmospheric Sciences and Climate, National Research Council/The National Academies, 500 Fifth St. NW, Washington, DC 20001.
E-mail: ikraucunas@nas.edu

tropical response to tropical forcing or the equatorward propagation of waves forced by midlatitude topography. The nondivergent barotropic vorticity equation provides a simpler framework for studying the propagation of wave activity through the extratropical upper troposphere and has been used extensively to study both the teleconnections associated with low-latitude forcing (e.g., Sardeshmukh and Hoskins 1988) and the horizontal dispersion of midlatitude wave trains (e.g., Watterson and Schneider 1987). A variety of linear and nonlinear three-dimensional models have also been used to simulate global stationary wave patterns with increasing realism (e.g., Hoskins and Rodwell 1995; Ting et al. 2001; Schumacher et al. 2004). Experiments with shallow-water models, on the other hand, have been restricted to studies of the subtropical dissipation of waves forced by midlatitude topography (e.g., Schneider and Watterson 1984; Brunet and Hayes 1996; Esler et al. 2000) or the evolution of transient disturbances in the Tropics (e.g., Webster and Chang 1988; Nieto Ferreira and Schubert 1999; Hsu and Plumb 2000).

One reason why the shallow-water equations have not been used more extensively to study tropical stationary waves is because specifying a realistic basic state can be problematic. The three methods commonly used to impose realistic basic states in shallow-water models are 1) linearizing the equations of motion about a specified basic state (e.g., Schneider and Watterson 1984), 2) specifying a zonally invariant mass source near the equator with corresponding mass sinks at higher latitude (e.g., Esler et al. 2000), or 3) initializing the model with balanced height and wind fields (e.g., Nieto Ferreira and Schubert 1999). The linear method is limited because both wave-wave and wave-mean flow interactions are precluded and are also difficult to justify because the eddy circulations at low latitudes are comparable in intensity to the mean flow. In addition, strong frictional drag is required to produce steady solutions in linear stationary wave models. This drag can be interpreted as a crude parameterization of the damping effects of nonlinear processes and transient eddies (Ting and Held 1990), but vorticity budgets (e.g., Sardeshmukh and Hoskins 1985) and axisymmetric models (e.g., Held and Hou 1980) suggest that the motions in the tropical upper troposphere are inherently nonlinear and inviscid.

The two methods used to impose realistic basic states in nonlinear shallow-water models, namely specifying a zonally invariant mass source/sink distribution or constructing a balanced basic state, suffer from a more subtle deficiency. To produce a basic-state zonal wind distribution with westerly midlatitude jetstreams, the

basic-state height field must be large in the Tropics (on the order of several kilometers) and decrease sharply toward the Poles. However, such a deep layer near the equator is inconsistent with the 15–250-m fluid depths implied by phase speed estimates for the first tropical baroclinic mode [$c = \sqrt{gh_o} \approx 12\text{--}50 \text{ m s}^{-1}$, Wheeler et al. (2000)] or the stability of an isentropic layer representing the Hadley cell outflow [$gh_o \sim 1000 \text{ m}^2 \text{ s}^{-2}$, Held and Phillips (1990)]. Hence, shallow-water models with basic states constructed using a mass source/sink distribution or a balancing procedure might be useful for studying extratropical waves, which are equivalent barotropic in structure, but are unsuitable for modeling tropical stationary waves.

In this paper, basic states are imposed in the nonlinear shallow-water system by specifying a thin (200 m) fluid layer over a large (1500 m), zonally symmetric topography distribution that decreases smoothly from the Tropics to the Poles. This configuration yields realistic basic-state winds without artificially enhancing tropical wave speeds or potential vorticity gradients, thus providing a consistent framework for studying eddy circulations at low latitudes. The idea of combining a shallow layer depth with a large meridional height gradient in the momentum equations was inspired by Held and Phillips (1990), who studied the influence of extratropical waves on the zonally averaged flow using a hybrid model in which the nondivergent barotropic vorticity equation was coupled to a modified shallow-water system.

As in previous shallow-water model experiments, stationary waves are generated by placing an isolated mass source at the equator, balanced by a weak mass sink at other longitudes. The influence of realistic basic-state winds on the stationary wave pattern is evaluated by comparing integrations performed using the topographically forced basic states with those performed in a resting basic state. The influence of hemispheric asymmetry on the response to tropical eddy forcing is explored by moving the mass source/sink distribution off the equator and by shifting the center of the zonal-mean topography field into one hemisphere to produce a “solstitial” basic state. The influence of the Hadley circulation on the stationary wave response is isolated by using a balancing procedure similar to that employed by Esler et al. (2000) and also by considering idealized perturbations to the linear barotropic vorticity equation.

The results of this study provide insight into several interesting features of the stationary waves in the tropical upper troposphere. Dima et al. (2005) recently noted that the eddy momentum fluxes associated with the seasonally varying large-scale waves in the equato-

rial upper troposphere are always directed opposite the prevailing mean meridional flow in the National Centers for Environmental Prediction–National Center for Atmospheric Research (NCEP–NCAR) reanalysis. Kraucunas and Hartmann (2005) noted a similar anticorrelation between the mean meridional circulation and eddy momentum fluxes over the equator in an idealized GCM forced with fixed tropical eddy heating. Our results indicate that hemispheric asymmetry in either the basic state or the eddy forcing gives rise to cross-equatorial eddy momentum fluxes and that the mean meridional flow amplifies these fluxes significantly when the eddy forcing and zonal-mean divergence are located in the same hemisphere. The stationary wave response also exhibits similar amplitudes on both sides of the equator when the eddy forcing resides in the summer hemisphere of the solstitial basic state, which suggests that the strong hemispheric symmetry of the tropical stationary wave pattern over the course of the seasonal cycle noted by Dima et al. (2005) can be attributed to the tendency for the maximum eddy and zonal-mean diabatic forcing to occur in the same latitude band.

The paper is organized as follows. The shallow-water equations are discussed in section 2. Our method for imposing zonally invariant basic states in the shallow-water system is introduced in section 3. The response of the model to steady eddy forcing at low latitudes is examined in section 4, with an emphasis on the influence of hemispheric asymmetry on both the equilibrium stationary wave structures and the eddy momentum fluxes near the equator. The final section summarizes our conclusions and includes some additional discussion of the relationship between the zonally averaged flow and steady eddy circulations at low latitudes.

2. Shallow-water equations

The following equations describe a thin, homogeneous layer of incompressible fluid with depth h under the influence of gravity, planetary rotation, and arbitrary forcing F on a spherical rotating planet with radius a , gravitational acceleration g , and planetary vorticity $f = 2\Omega \sin\theta$. The total height field H is the sum of the fluid depth h and surface topography h_s ($H = h + h_s$):

$$\frac{\partial u}{\partial t} = f v - \frac{u}{a \cos\theta} \frac{\partial u}{\partial \lambda} - \frac{v}{a} \frac{\partial u}{\partial \theta} + \frac{uv \tan\theta}{a} - \frac{g}{a \cos\theta} \frac{\partial H}{\partial \lambda} + F_u, \quad (1)$$

$$\frac{\partial v}{\partial t} = -f u - \frac{u}{a \cos\theta} \frac{\partial v}{\partial \lambda} - \frac{v}{a} \frac{\partial v}{\partial \theta} - \frac{u^2 \tan\theta}{a} - \frac{g}{a} \frac{\partial H}{\partial \theta} + F_v, \quad (2)$$

$$\frac{\partial h}{\partial t} = -\frac{u}{a \cos\theta} \frac{\partial h}{\partial \lambda} - \frac{v}{a} \frac{\partial h}{\partial \theta} - \frac{h}{a \cos\theta} \frac{\partial u}{\partial \lambda} - \frac{h}{a} \frac{\partial v}{\partial \theta} + F_h. \quad (3)$$

It is often convenient to express these equations in vorticity–divergence form, using the absolute vorticity $\xi = f + \zeta$ and kinetic energy per unit mass $K = (u^2 + v^2)/2$:

$$\frac{\partial \xi}{\partial t} = \frac{\partial \zeta}{\partial t} = -\xi \delta - \frac{u}{a \cos\theta} \frac{\partial \zeta}{\partial \lambda} - \frac{v}{a} \frac{\partial \zeta}{\partial \theta} + F_\zeta, \quad (4)$$

$$\frac{\partial \delta}{\partial t} = -\frac{1}{a \cos\theta} \frac{\partial(\xi v)}{\partial \lambda} - \frac{\partial(\xi u)}{a \partial \theta} - \nabla^2(K + gH) + F_\delta, \quad (5)$$

$$\frac{\partial h}{\partial t} = -h \delta - \frac{u}{a \cos\theta} \frac{\partial h}{\partial \lambda} - \frac{v}{a} \frac{\partial h}{\partial \theta} + F_h. \quad (6)$$

In the absence of forcing, the shallow-water equations conserve potential vorticity ($\eta = \xi/h$), potential enstrophy ($\eta^2/2$), and (globally) total energy. Also note that the only place where topography enters the system (4)–(6) is through the Laplacian term in the divergence equation [or, in (1)–(3), through the derivatives of the total height field in the momentum equations].

The numerical model that we use to integrate the shallow-water equations is the Geophysical Fluid Dynamics Laboratory (GFDL) “FMS” shallow-water model. This model employs the vorticity–divergence form of the shallow-water equations (4)–(6), with linear terms computed using a spectral transform method and nonlinear terms calculated on the corresponding Gaussian grid. Time differencing is treated semi-implicitly, with a Robert–Asselin filter. The experiments described in this paper were performed at T42 resolution with a ∇^8 hyperdiffusion that damps the smallest resolved features at a time scale of roughly 1 day. Our results are not sensitive to these aspects of the model.

3. Basic states

In the shallow-water system, mass sources and sinks play a role analogous to diabatic heating and cooling, respectively, in a stratified atmosphere and may be imposed by imposing a fixed mass source/sink Q , relaxing the height field toward a reference height field h_{ref} , or both:

$$F_h = Q(\lambda, \theta) - k_h \{h - h_{\text{ref}}(\lambda, \theta)\}. \quad (7)$$

A basic-state circulation resembling the mean flow in the upper troposphere can be generated using (7) by imposing a zonally invariant mass source near the equator with compensating mass sinks at higher latitudes or

by relaxing the height field toward a zonally invariant reference height distribution that is large near the equator and decreases toward the Poles. The other method commonly used to impose realistic basic states in nonlinear shallow-water models is to specify the desired wind distribution and use a balancing procedure to obtain an initial height field using the nonlinear balance equation:

$$g\nabla^2 h_{\text{bal}} = \frac{1}{a \cos\theta} \frac{\partial(\xi v)}{\partial\lambda} - \frac{\partial(\xi u \cos\theta)}{a \cos\theta} \frac{\partial}{\partial\theta} - \nabla^2 K. \quad (8)$$

As discussed in the introduction, the basic-state height fields generated using either (7) or (8) must be large in the Tropics in order to produce realistic upper-tropospheric winds, but a deep fluid layer at the equator is inconsistent with the shallow equivalent depths implied by the slow phase speeds and weak static stabilities observed in the tropical troposphere. To circumvent this problem, we consider a thin fluid layer sitting on top of a zonally symmetric topography distribution with the following form:

$$h_s = H_0 \{1 - (\sin\theta - \sin\theta_0)^2\}. \quad (9)$$

Here H_0 represents the maximum height of the topography, θ_0 is the latitude where this peak occurs, and the sine-squared profile provides a meridional gradient that approximates the observed upper-tropospheric geopotential height gradient. Hemispherically symmetric basic states are created when $\theta_0 = 0^\circ$. Solstitial basic states are generated when θ_0 is nonzero; the hemisphere containing the peak of the topography will have smaller meridional height gradients and weaker zonal-mean zonal winds, and thus corresponds to the “summer” hemisphere on Earth.

To generate a mean meridional circulation and prevent the fluid from simply “running down” the mountain, the fluid depth is relaxed toward its initial, global-mean value h_0 :

$$F_h = -(h - h_0)/\tau. \quad (10)$$

In all of the experiments below, we use a thermal damping time scale of $\tau = 10$ days and an initial global-mean fluid depth of $h_0 = 200$ m. In equilibrium, the mean fluid depth will be lower than h_0 near the equator and larger than h_0 away from the equator, so (10) gives rise to a mean meridional flow analogous to the outflow from the Hadley circulation.

Some form of frictional drag is usually included in the zonal momentum equation in order to balance the Coriolis accelerations associated with the mean meridional circulation and to permit steady solutions when eddy

forcing is added. We use a linear drag for both the zonal and meridional velocities:

$$\begin{aligned} F_u &= -ku \\ F_v &= -kv. \end{aligned} \quad (11)$$

In most of the experiments described below, the strength of the frictional drag is the same as the damping strength used in the height equation [i.e., $k = 1/\tau = (10 \text{ days})^{-1}$]. Since the tropical upper troposphere is generally regarded as a region with weak frictional drag and long thermal damping time scales, we would prefer to use even weaker frictional drag and thermal damping along with a smaller fluid depth. However, in the presence of realistic eddy forcing, fluid depths less than 200 m give rise to Froude numbers ($F = 2K/gh$) approaching unity.

Figure 1 shows the topography distributions and zonally symmetric climates produced by the shallow-water model described in section 2 forced using (9)–(11) with $k = 1/\tau = (10 \text{ days})^{-1}$ and $H_0 = 1500$ m. The $\theta_0 = 0^\circ$ case (solid lines) is referred to as the “equinoctial” basic state, while the $\theta_0 = 5^\circ$ run corresponds to the solstitial basic state. To prevent negative fluid depths near the Pole in the solstitial basic state, a horizontally uniform bias of 200 m is added to the topography distribution in both experiments; this offset does not affect the results since the horizontal height gradients remain unchanged. Integrations are initialized using a resting fluid with uniform depth $h_0 = 200$ m, and the zonally symmetric topography is raised over the first 25 days of each experiment. The equilibrium response is typically established after 50 days. The results presented below are from day 200.

The equilibrium zonal and meridional winds in the equinox basic state (solid lines in Figs. 1d,e) bear a strong resemblance to the observed zonally averaged flow in the upper troposphere during equinox months (see, e.g., Dima et al. 2005). The solstitial basic state (dashed lines) likewise provides a reasonable facsimile of the observed upper-tropospheric flow during austral winter, with stronger zonal winds in the “winter” hemisphere, weaker zonal flow in the summer hemisphere, and a mean meridional circulation dominated by a single Hadley cell straddling the equator. The conservation of angular momentum following the cross-equatorial flow gives rise to easterly zonal winds at the equator in the solstitial basic state (cf. Lindzen and Hou 1988). In both basic states, the equilibrium fluid depth (Fig. 1c) is ~ 100 m near the equator, which is within the appropriate range for simulating the equatorial waves discussed above. The fluid depth increases to ~ 250 m at $\sim 15^\circ\text{N}$, then gradually decreases to ~ 220 m at the

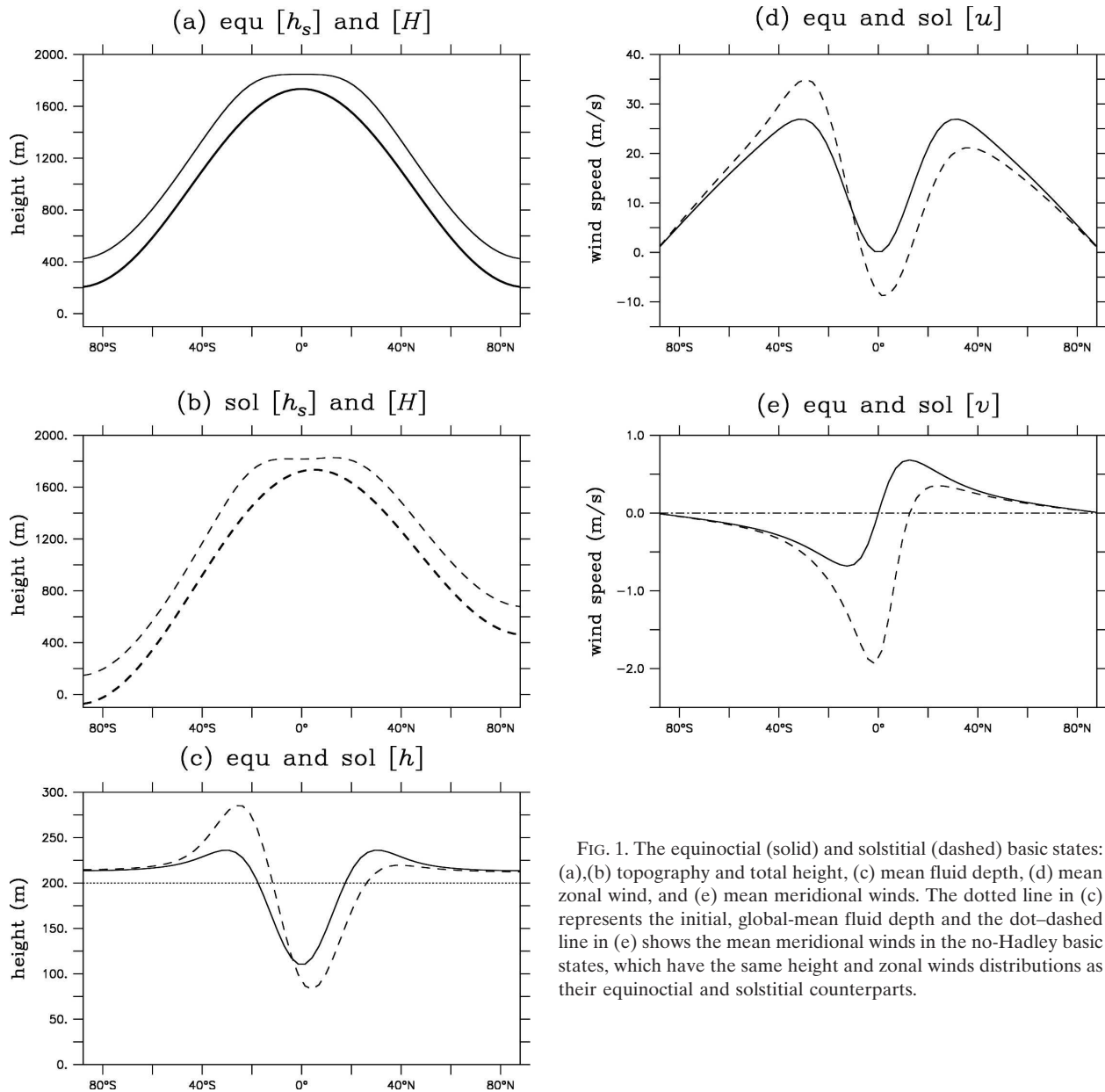


FIG. 1. The equinoctial (solid) and solstitial (dashed) basic states: (a),(b) topography and total height, (c) mean fluid depth, (d) mean zonal wind, and (e) mean meridional winds. The dotted line in (c) represents the initial, global-mean fluid depth and the dot-dashed line in (e) shows the mean meridional winds in the no-Hadley basic states, which have the same height and zonal winds distributions as their equinoctial and solstitial counterparts.

Poles. These depths are too small to permit extratropical wave trains to develop in response to tropical forcing (cf. Lau and Lim 1984).

Basic-state experiments with different values for k and τ (not shown) indicate a similar sensitivity to thermal and frictional damping strength as Held and Phillips (1990), who found that the mean zonal wind distribution in a similar but slightly simpler model depends on the damping parameters and fluid depth only through the combination $h_0 k_f k_f^{-1}$, while the mean meridional flow approaches a lower bound proportional to $k_f h_0^{-1}$ as $k_f \rightarrow 0$. Experiments with a momentum source

proportional to the tropical mass source (Gent 1993) produce basic states similar to those depicted in Fig. 1 and exhibit a response to tropical eddy forcing similar to that described in the next section.

To isolate the influence of the Hadley circulation on the tropical stationary waves induced by steady thermal forcing near the equator, we also consider zonally symmetric basic states that do not have a mean meridional circulation, but are otherwise identical to the equinoctial and solstitial basic states. These “no Hadley” basic states are generated by solving the nonlinear balance Eq. (8) with the meridional winds set equal to zero and

the zonal winds set equal to one of the equilibrium zonal wind fields generated using (9)–(11). The topography distribution is then set equal to the difference between the balanced height field and the equilibrium total height field from the corresponding full basic-state integration. Since the general circulation is usually very close to nonlinear balance and the mean meridional winds are much weaker than the mean zonal winds, this procedure yields topography fields that are nearly identical to those produced using (9)–(11). When eddy forcing is present, the wind and height perturbations in the no Hadley experiments are relaxed toward their initial, zonally symmetric values with the same (10 days)^{−1} damping used in the equinoctial and solstitial experiments.

4. Response to eddy forcing

In this section, we examine the response of the shallow-water model described in the previous section to a zonally asymmetric mass source/sink distribution given by

$$Q^*(\lambda, \theta) = Q_e \exp \left\{ - \left(\frac{\lambda - \lambda_e}{\Delta\lambda} \right)^2 - \left(\frac{\theta - \theta_e}{\Delta\theta} \right)^2 \right\} - \bar{Q}(\theta). \quad (12)$$

The mass source is centered at the date line ($\lambda_e = 180^\circ$) with a longitudinal scale of $\Delta\lambda = 30^\circ$, a latitudinal scale of $\Delta\theta = 5^\circ$, and an amplitude of $Q_e = 100 \text{ m day}^{-1}$. The damping in the model permits a steady-state solution. To study the effects of hemispherically asymmetric forcing, experiments are performed with the mass forcing centered at either the equator ($\theta_e = 0^\circ$) or at 10°N . Here \bar{Q} represents the zonal average of the mass source, which is removed in order to prevent the direct forcing of a zonal-mean response.

The model is initialized with the equinoctial basic state, the solstitial basic state, one of the corresponding no-Hadley basic states, or a resting basic state constructed by specifying zero topography everywhere ($h_s \equiv 0$) and a fluid depth of 100 m, which approximates the equilibrium depth near the equator in the realistic basic states (Fig. 1c). The eddy forcing is increased linearly over the first 25 days of each run, and the equilibrium response is typically established by day 75. Results shown below are from day 200. Identical results are obtained for any balanced initial state. The zonal-mean component of the response is generally small due to the removal of the zonal mean in (12), and has been removed from all of the figures below in order to focus on the steady eddy circulation. The small zonal-mean

zonal wind response of the shallow-water model to imposed eddy forcing is discussed in detail in Kraucunas (2005).

To identify the factors controlling the zonally asymmetric response to tropical eddy forcing and the changes induced by imposing hemispheric asymmetry and/or realistic basic states, it is useful to consider the eddy vorticity balance, which may be written:

$$\frac{\partial \zeta^*}{\partial t} = -(\xi\delta)^* - (\mathbf{v}_i^* \cdot \nabla \xi)^* - (\mathbf{v}_r^* \cdot \nabla \xi)^* - \frac{[u]}{a \cos\theta} \frac{\partial \zeta^*}{\partial \lambda} - \frac{[v]}{a} \frac{\partial \zeta^*}{\partial \theta} - (k\zeta)^* \approx 0. \quad (13)$$

The subscripts r and i in (13) denote the rotational and irrotational (divergent) components of the equilibrium eddy circulation, respectively, while brackets and asterisks denote zonally averaged and zonally asymmetric (eddy) quantities. Note that the absolute vorticity ξ is the sum of the planetary vorticity f , the eddy vorticity ζ^* , and the zonal-mean relative vorticity $[\zeta]$ associated with the zonal-mean zonal wind field.

a. Resting basic-state solutions

Figure 2 shows the equilibrium eddy responses obtained when the shallow-water model is integrated with eddy forcing centered both on and off the equator in a resting basic state. The height and wind anomalies in the hemispherically symmetric solution (Fig. 2a) are analogous to those found in the linear response to an isolated mass sink studied by Gill (1980). However, the compensating mass sink in (13), along with the relatively weak damping and periodic domain of our model, gives rise to a solution that bears a closer resemblance to the zonal wavenumber-one response obtained by Matsuno (1966). The ridge in the height field along the equator and the dividing line between easterly and westerly flow are located slightly to the east of the maximum forcing, while the strongest eddy zonal winds and negative height anomalies are found to the west of the mass source. The equilibrium eddy vorticity field in the hemispherically symmetric experiment (Fig. 2b) is dominated by a pair of anticyclones straddling the equator to the west of the mass source. The strong easterly winds to the west of the mass source in Fig. 2a are clearly associated with the rotational flow around these anticyclones, and the meridional winds are directed toward (away from) the equator in the mass source (sink) region to complete the nondivergent circulation. The eddy divergence field (shading in Fig. 2c) is virtually identical in structure to the mass forcing,

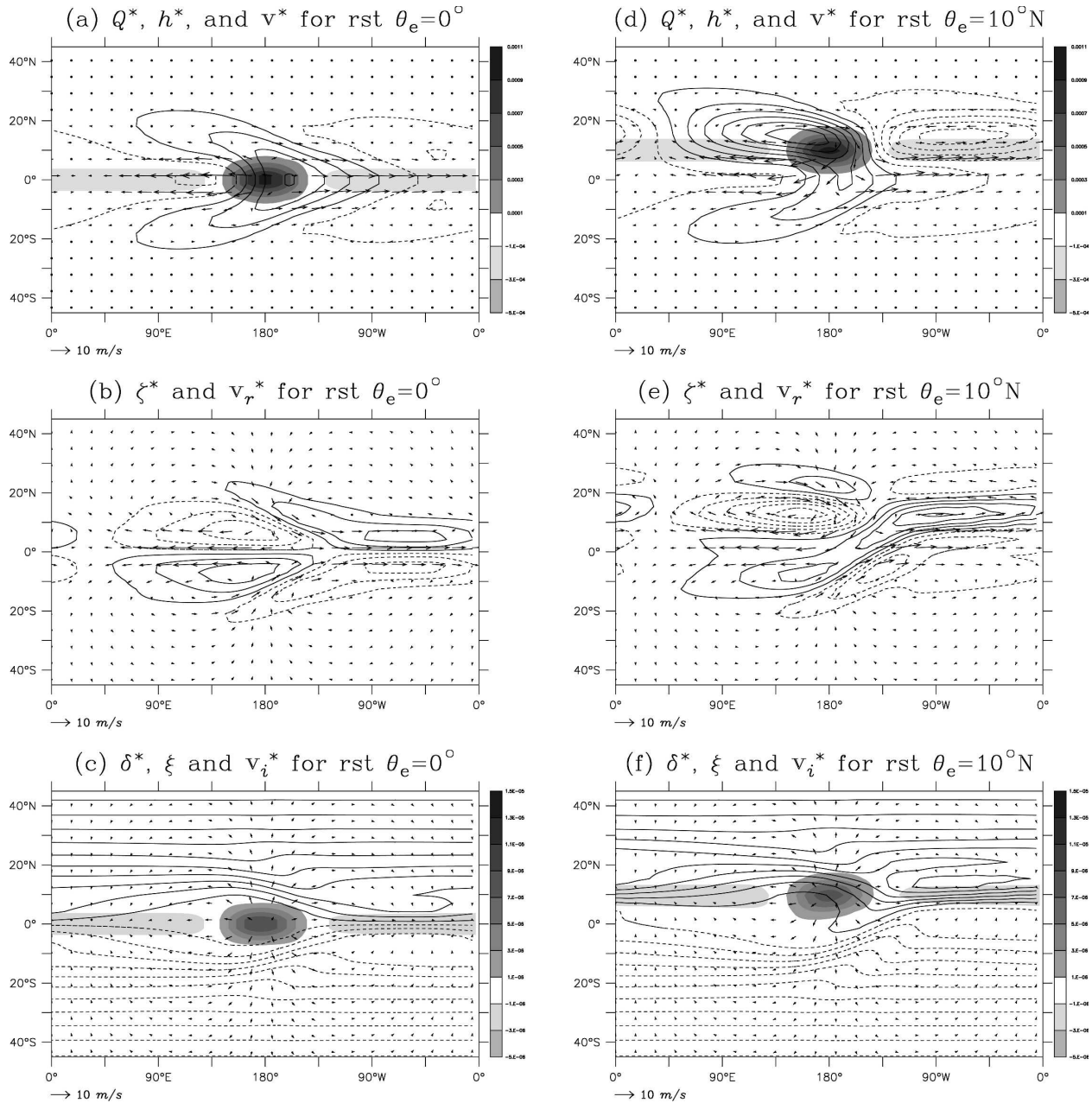


FIG. 2. The equilibrium eddy response in the (a)–(c) $\theta_e = 0^\circ$ and (d)–(f) $\theta_e = 10^\circ\text{N}$ resting basic-state experiments: (a), (d) eddy height field (contours every 5 m), mass source (shading every $2 \times 10^{-4} \text{ m s}^{-1}$), and eddy winds (vectors); (b), (e) eddy vorticity (contours every $5 \times 10^{-6} \text{ s}^{-1}$) and eddy rotational winds (vectors); and (c), (f) absolute vorticity (contours every $1 \times 10^{-5} \text{ s}^{-1}$), eddy divergence (shading every $2 \times 10^{-4} \text{ s}^{-1}$), and eddy divergent winds (vectors).

which is the shallow-water analog of the balance between eddy heating and vertical motion in the tropical atmosphere (see, e.g., Schumacher et al. 2004). The divergent winds (vectors in Fig. 2c) reinforce the rotational winds along the equator but tend to cancel the rotational flow in both hemispheres, for reasons that are discussed below.

Figure 3 shows the eddy vorticity balance (13) for the

resting basic-state experiment with eddy forcing at the equator (the terms involving the zonal-mean winds are negligible in the resting basic state). The dominant balance is between the generation of vorticity by divergent advection (Fig. 3b) and the advection of vorticity by the rotational winds (Fig. 3c), with divergence forcing and frictional drag only making small contributions near the equator. The equilibrium divergence forcing is weak

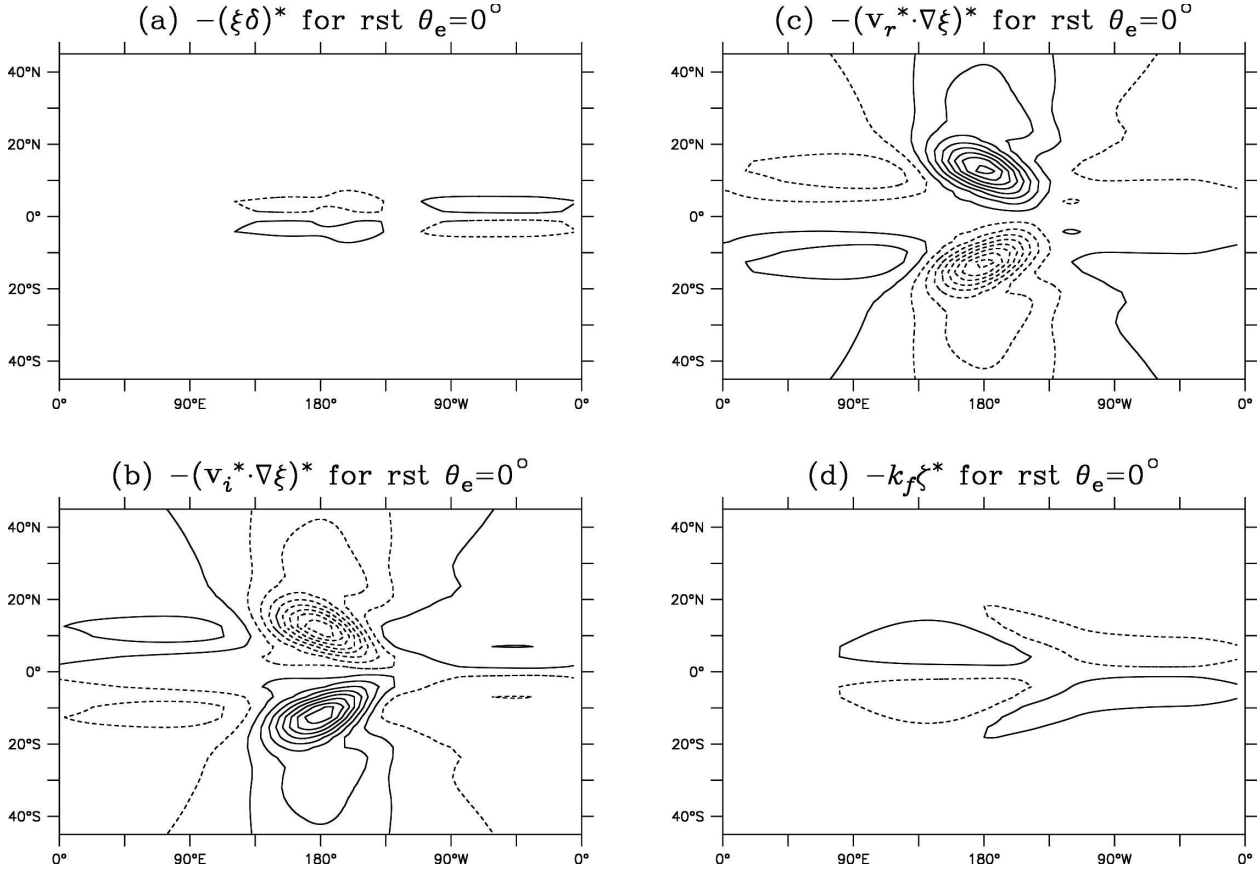


FIG. 3. Vorticity balance components for the $\theta_e = 0^\circ$ resting basic-state experiment: contours every $1.5 \times 10^{-11} \text{ s}^{-2}$.

because the finite anticyclonic vorticity anomalies in the mass source region reduce the local vorticity gradient over time; this “pool of zero absolute vorticity” (Hoskins et al. 1999) can be seen at, and to the west of, the divergence anomaly in Fig. 2c. Divergent advection, on the other hand, provides significant anticyclonic forcing because the eddy divergent winds are much broader than the eddy divergence or eddy vorticity anomalies (see Fig. 2e), and are generally oriented orthogonal to the vorticity field, as discussed by Sardeshmukh and Hoskins (1988). Hence, we can infer that the Rossby wave response increases in amplitude until eddy vorticity advection (plus frictional drag) balances the forcing associated with the eddy divergence and divergent winds. This balance between rotational and divergent vorticity advection explains why the eddy circulations are weak away from the equator and also why the Rossby gyres are centered to the west of the mass source. The westward displacement of the Rossby gyres relative to the eddy forcing is also consistent with the westward group velocity of Rossby waves (Gill 1980).

Moving the eddy forcing off the equator (Figs. 2d–f) leads to a significant amplification, and slight north-

ward shift, in the eddy height and vorticity anomalies in that hemisphere. However, the response in the Southern Hemisphere remains comparable in intensity to the response in the hemispherically symmetric case despite the fact that the eddy divergence anomaly induced by the mass source resides entirely north of the equator. The overall increase in rotational flow leads to slightly stronger eddy zonal winds along the equator, and the latitudinal displacement of the eddy forcing gives rise to eddy divergent winds that are directed across the equator, especially to the south of the mass source. This cross-equatorial eddy divergent flow, combined with the slight eastward bias in the dividing line between easterly and westerly winds, leads to a noticeable southwest–northeast tilt in the eddy wind vectors along the equator, implying a northward flux of eddy momentum. Dima et al. (2005) report similar results using a shallow-water model forced in a similar manner and show that the observed seasonally varying stationary waves in the tropical upper troposphere also exhibit cross-equatorial eddy momentum fluxes and substantial hemispheric symmetry throughout the year. Lau and Lim (1984) noted that tilted eddy circulations are also generated

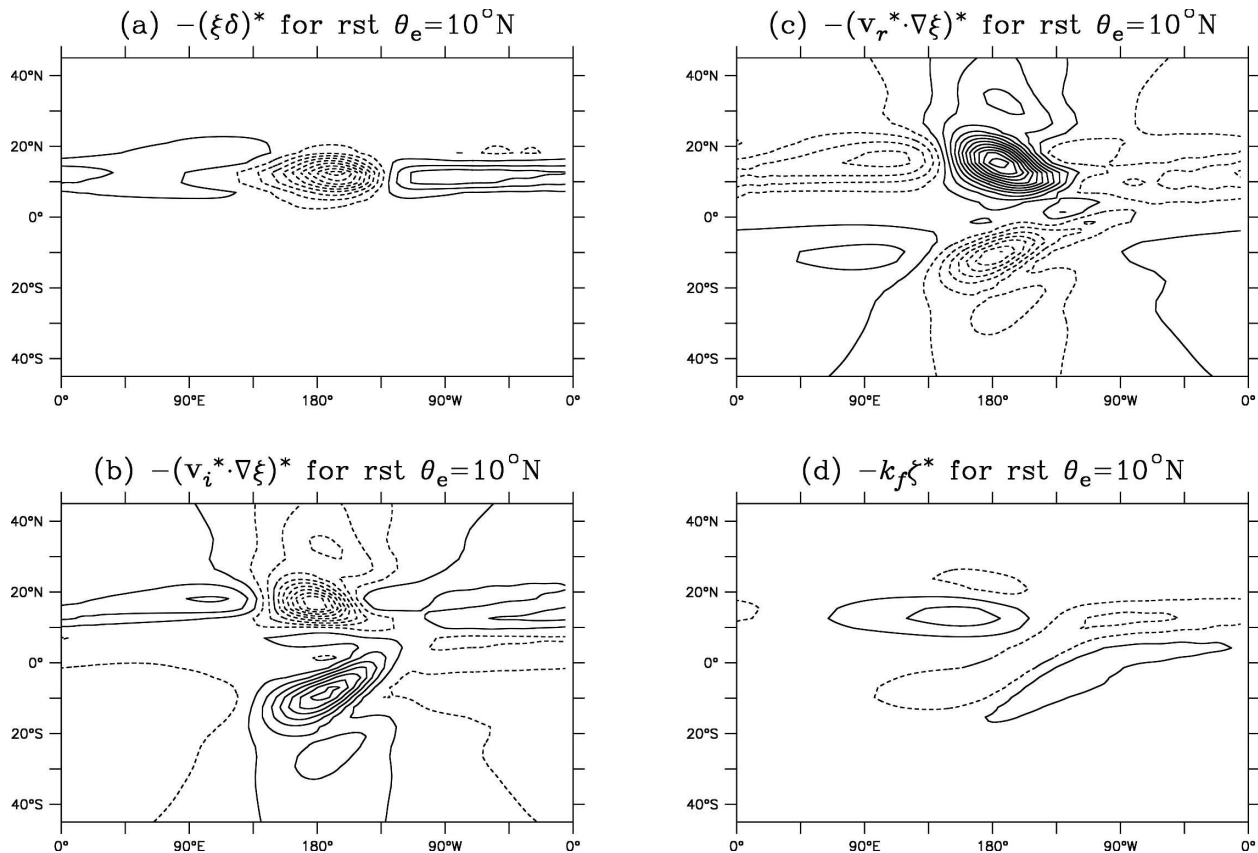


FIG. 4. As in Fig. 3 except for the $\theta_e = 10^\circ\text{N}$ resting basic-state experiment.

when mass forcing is imposed farther away from the equator (27° and 35°N) in a shallow-water model, but the observed eddy diabatic forcing is generally located closer to the equator.

The eddy vorticity balance for the resting basic-state experiment with hemispherically asymmetric forcing (Fig. 4) indicates that the amplification of the response in the forced hemisphere may be attributed to an increase in divergent forcing (Fig. 4a), which in turn may be attributed to the increase in planetary vorticity with latitude and the latitudinal displacement of the mass source outside the “pool of zero vorticity” near the equator. The reason why the Southern Hemisphere response only weakens slightly when the eddy forcing is moved into the Northern Hemisphere, on the other hand, is because the eddy divergent winds continue to provide significant anticyclonic vorticity advection on the other side of the equator (Fig. 4b). Sardeshmukh and Hoskins (1988) ascribe the hemispheric symmetry of the extratropical response to tropical eddy forcing to a similar effect. Also note that the cross-equatorial eddy divergent winds to the south of the mass source do not give rise to a rotational response because the vor-

ticity gradient is small near the equator. We will discuss the eddy momentum fluxes implied by the tilted eddy wind field along the equator in section 4d.

b. Equinoctial basic-state solutions

Figure 5 shows the equilibrium zonally asymmetric response of the shallow-water model integrated with eddy forcing both on and off the equator in the equinoctial basic state. The eddy height field in the $\theta_e = 0^\circ$ experiment (Fig. 5a) is dominated by large positive anomalies centered almost directly north and south of the mass source (note that the contour interval in Fig. 5a is twice as large as in Fig. 2a). The easterly eddy zonal winds near the equator are also stronger and extend farther into each hemisphere than the easterly wind anomalies in the resting basic state, while the westerly wind anomalies to the east of the mass source are slightly weaker. In addition, the height anomalies and the dividing line between easterly and westerly flow along the equator have both shifted to the east so that easterly flow now dominates the mass source region. The eddy vorticity anomalies and rotational winds (Fig. 5b) are also centered eastward and poleward of

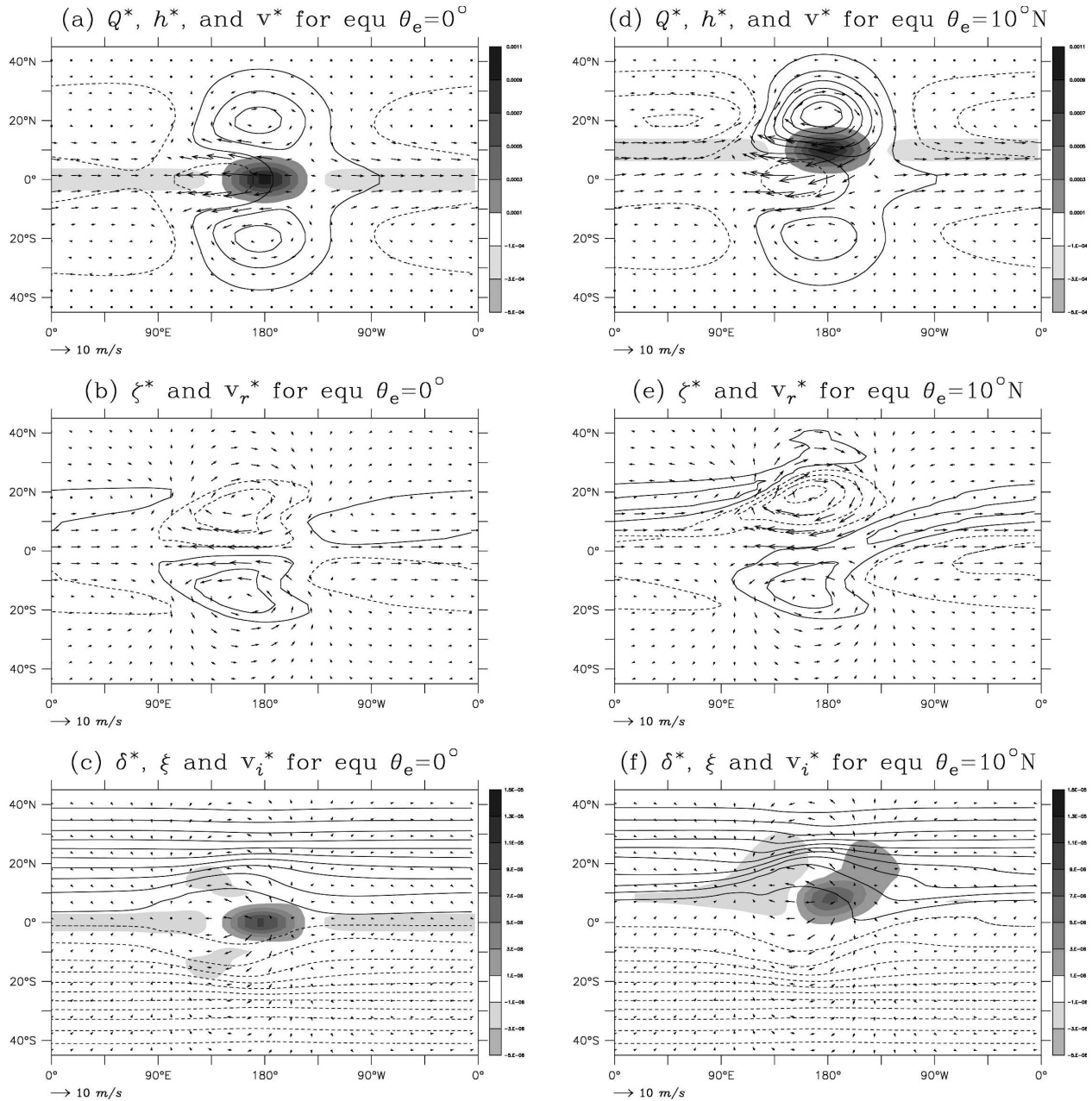


FIG. 5. As in Fig. 2 except for the equinoctial basic state: contour interval is 10 m in (a) and (d).

their positions in the resting basic state (Fig. 2b). All of these changes bring the eddy circulation much closer to the observed quasi-stationary wave pattern in the tropical upper troposphere on earth during spring and autumn (e.g., Dima et al. 2005), which suggests that the inclusion of a realistic basic state is crucial for accurately simulating the climatological steady eddy circulation in the tropical band.

Figure 6 shows the eddy vorticity balance for the equinoctial run with eddy forcing centered at the equator.

As in the resting basic state, the formation of a pool of zero absolute vorticity limits the forcing associated with the eddy divergence anomaly in the mass source region (Fig. 6a). The broader scale of the anticyclonic vorticity anomalies in Fig. 5, combined with the weaker absolute vorticity gradient on the equatorward side of the subtropical jets in the equinoctial basic state, also leads to a slight reduction in vorticity advection by the eddy divergent winds in the tropical band (Fig. 6b). However, the westerly zonal-mean flow enhances the

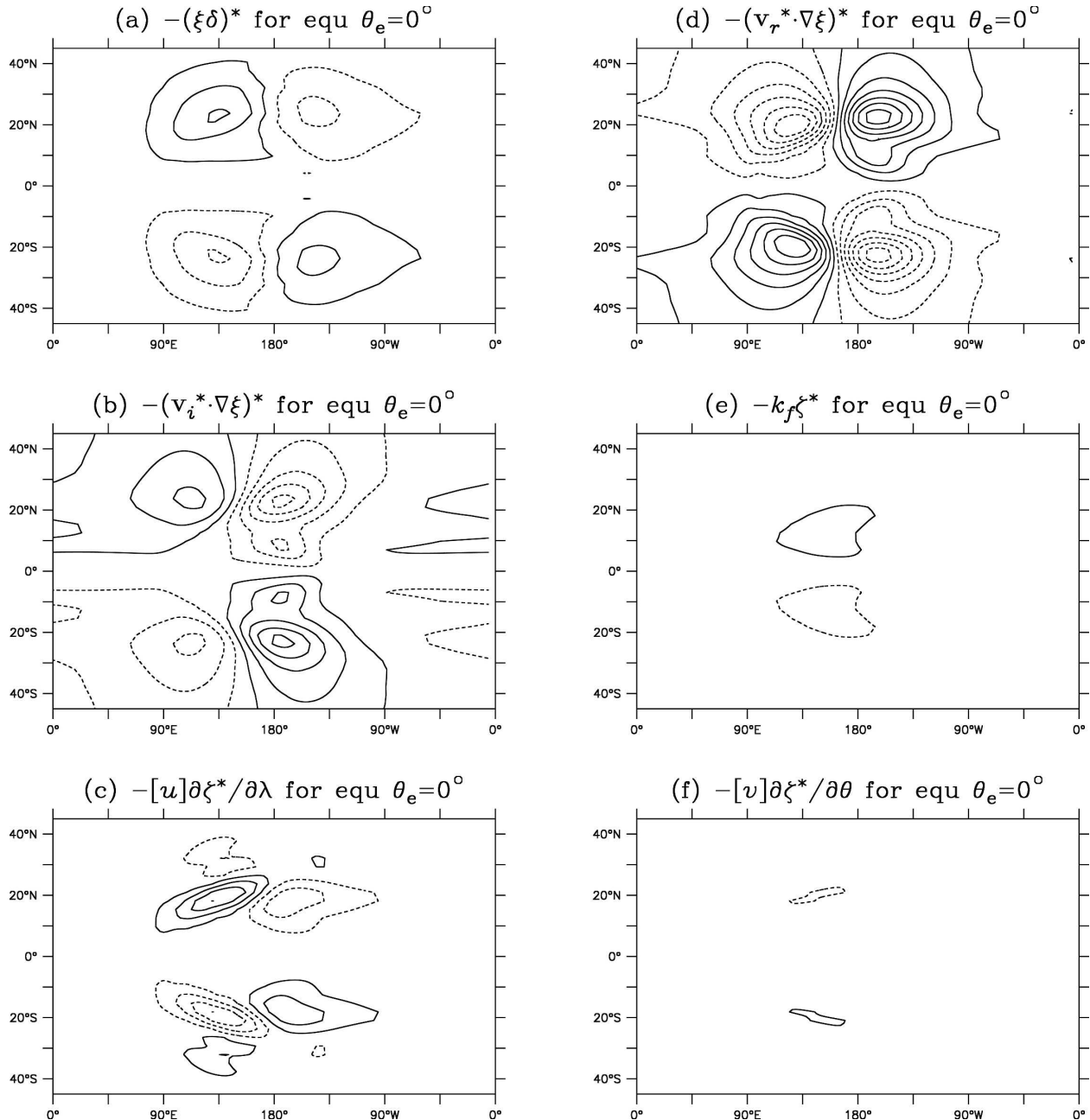


FIG. 6. As in Fig. 3 except for the equinoctial $\theta_e = 0^\circ$ experiment and including the zonal-mean wind terms.

meridional propagation of Rossby wave activity and also tends to retard the westward propagation of the wave somewhat (Philips and Gill 1987), while the advection of vorticity by the westerly zonal-mean flow acting on the eddy vorticity anomalies (Fig. 6c) reinforces the anticyclonic vorticity generation poleward and eastward of the mass source. Figure 6a indicates that isolated divergence and convergence anomalies in the subtropics also tend to reinforce the anticyclonic circulation to the east of the mass source, and provide

cyclonic forcing to the west. Experiments with a fixed eddy divergence field (not shown) indicate that these isolated subtropical divergence anomalies, which are partially visible in Fig. 5c (the divergence anomalies to the east of the mass source are not quite large enough to show up) are induced by the advection of vorticity by the rotational flow to the west and east of the mass source (Fig. 6d), which is no longer balanced by divergent advection alone. The advection of vorticity by the mean meridional winds (Fig. 6f), on the other hand, has

little influence on the vorticity balance in the equinoctial basic state.

As in the resting basic state, moving the eddy forcing off the equator (Figs. 5d–f) amplifies the response in the hemisphere with the forcing and leads to a tilt in the eddy wind vectors along the equator, with only a slight decrease in amplitude in the opposite hemisphere. An analysis of the eddy vorticity balance (not shown) confirms that the amplification of the eddy response arises from the displacement of the eddy divergence forcing into a region with stronger absolute vorticity, that the westerly zonal-mean zonal winds in the subtropics of the equinoctial basic state are responsible for amplifying the eddy response relative to the corresponding resting basic state integration, and that the westerly zonal-mean flow and induced subtropical eddy divergence anomalies are responsible for shifting the centers of the Rossby gyres to the east.

c. Solstitial basic-state solutions

Figure 7 shows the response of the shallow-water model to eddy forcing on and off the equator in the solstitial basic state. When the forcing is centered at the equator (Figs. 7a–c), the wind and height variations in the Northern (summer) Hemisphere are much weaker than the corresponding features in the equinoctial basic state (Fig. 5a), while the eddy response in the Southern (winter) Hemisphere is enhanced. Also note that the strongest eddy winds and the dividing line between clockwise and counterclockwise rotation (Fig. 7b) are both located slightly south of the equator, while the eddy divergence and divergent winds (Fig. 7c) remain collocated with the mass forcing at zero latitude (although the divergence anomalies induced by the rotational flow in the Southern Hemisphere are somewhat stronger). This latitudinal separation between the rotational and divergent components of the circulation gives rise to a northeast–southwest tilt in the eddy wind vectors near the equator, as in the equinoctial experiment with eddy forcing off the equator, although in this case the strongest wind anomalies are now found slightly south of the equator.

The vorticity balance in the solstitial $\theta_e = 0^\circ$ run, shown in Fig. 8, indicates that the hemispheric asymmetry of the eddy response in the solstitial basic state can be attributed mostly to the hemispheric asymmetry of the zonal-mean zonal wind field: the strong westerly zonal-mean flow in the winter hemisphere amplifies the Rossby wave response and provides strong zonal vorticity advection (Fig. 8c). However, the cross-equatorial mean meridional winds in the solstitial basic state (cf. Fig. 2e) are associated with substantial vorticity advection in the vicinity of the equator (Fig. 8f), which ap-

pears to be responsible for the southward shift in the dividing line between clockwise and counterclockwise rotation in Fig. 7b (Fig. 8a indicates that the divergence anomaly associated with the mass source also tends to reinforce the counterclockwise motion once the zero vorticity line shifts south of the equator). The zonal-mean divergence field associated with the cross-equatorial mean meridional flow in the solstitial basic state also tends to reduce the amplitude of the eddy vorticity anomalies in the Northern Hemisphere and enhance the vorticity anomalies south of the equator, although this effect is only responsible for a small fraction of the hemispheric asymmetry in Figs. 7a,b.

As in the equinoctial and resting basic states, moving the mass forcing north of the equator in the solstitial basic state (Figs. 7d–f) enhances in the eddy response in the Northern Hemisphere dramatically with only a slight reduction in the eddy response in the Southern Hemisphere. However, since the Southern Hemisphere response is already quite strong in the solstitial basic state, the eddy response in the solstitial $\theta_e = 10^\circ\text{N}$ experiment is stronger than any other experiment, and the eddy height and vorticity anomalies are almost symmetric about the equator. This result suggests that strength and hemispheric symmetry of the eddy circulations in the tropical upper troposphere during solstitial months noted by Dima et al. (2005) may be attributed to the tendency for the maximum eddy and zonal-mean diabatic forcing to occur on the same side of the equator. The strength of the eddy response in the summer hemisphere can be attributed to the displacement of the eddy forcing into a region with a larger absolute vorticity (and vorticity gradient), while the strong response in the winter hemisphere arises due to the stronger zonal-mean flow on that side of the equator. Experiments with a linearized version of the model (Kraucunas 2005) indicate that nonlinear effects, especially the nonlinear advection of vorticity by the rotational and divergent flows, are also important in the solstitial $\theta_e = 10^\circ\text{N}$ experiment, especially where the easterly zonal-mean flow tends to amplify the easterly eddy winds near the equator.

Watterson and Schneider (1987) determined that cross-equatorial mean meridional winds enhance the propagation of wave activity in the direction of the flow and retard wave propagation in the opposite direction, in accordance with group velocity considerations. Their analysis suggested that this effect is particularly evident when the mean zonal winds at the equator are easterly. To determine if this effect operates in our model, the $\theta_e = 0^\circ$ and $\theta_e = 10^\circ\text{N}$ eddy forcing experiments were repeated using the solstitial no-Hadley basic states described in the previous section. Figure 9 shows the equi-

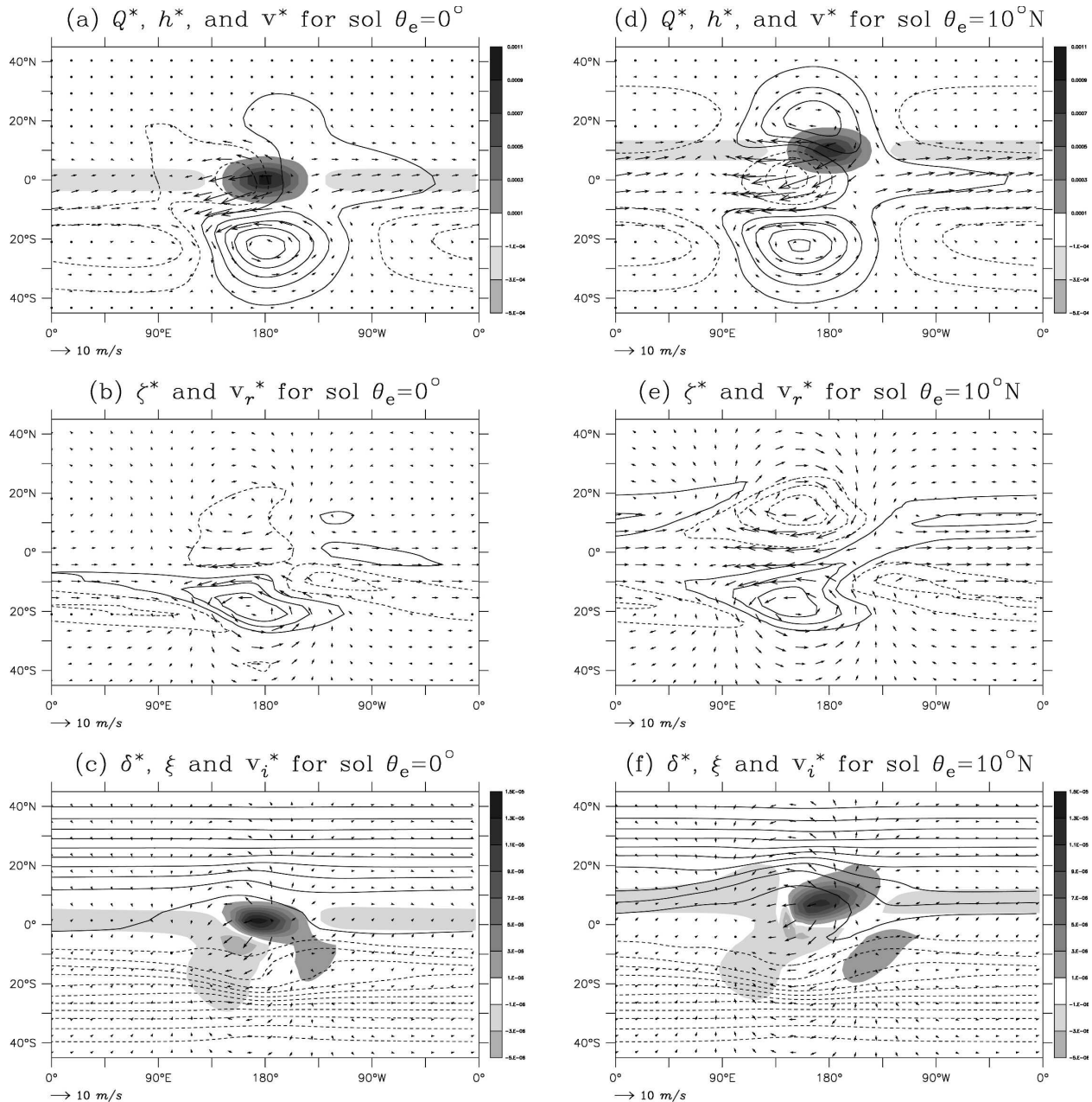


FIG. 7. As in Fig. 5 except for the solstitial basic state.

librium eddy response of these two no-Hadley experiments. The differences between Figs. 9a and 7a are relatively small, but Fig. 9b shows a much weaker eddy response south of the equator than Fig. 7b, indicating that the cross-equatorial mean meridional flow indeed plays an important role in promoting a hemispherically symmetric eddy response in the solstitial basic state when the eddy forcing is centered in the summer hemisphere. The eddy winds near the equator in Fig. 9b are also slightly weaker and exhibit a less pronounced

northeast–southwest tilt than those in Fig. 7b. As discussed in the next section, these changes in the eddy wind field have a significant impact on the transport of momentum across the equator.

d. Tropical eddy momentum fluxes

The zonally averaged eddy momentum fluxes in the equinoctial, equinoctial no-Hadley, solstitial, and solstitial no-Hadley experiments are plotted in Fig. 10. These fluxes arise due to the tilt in the eddy wind vectors that

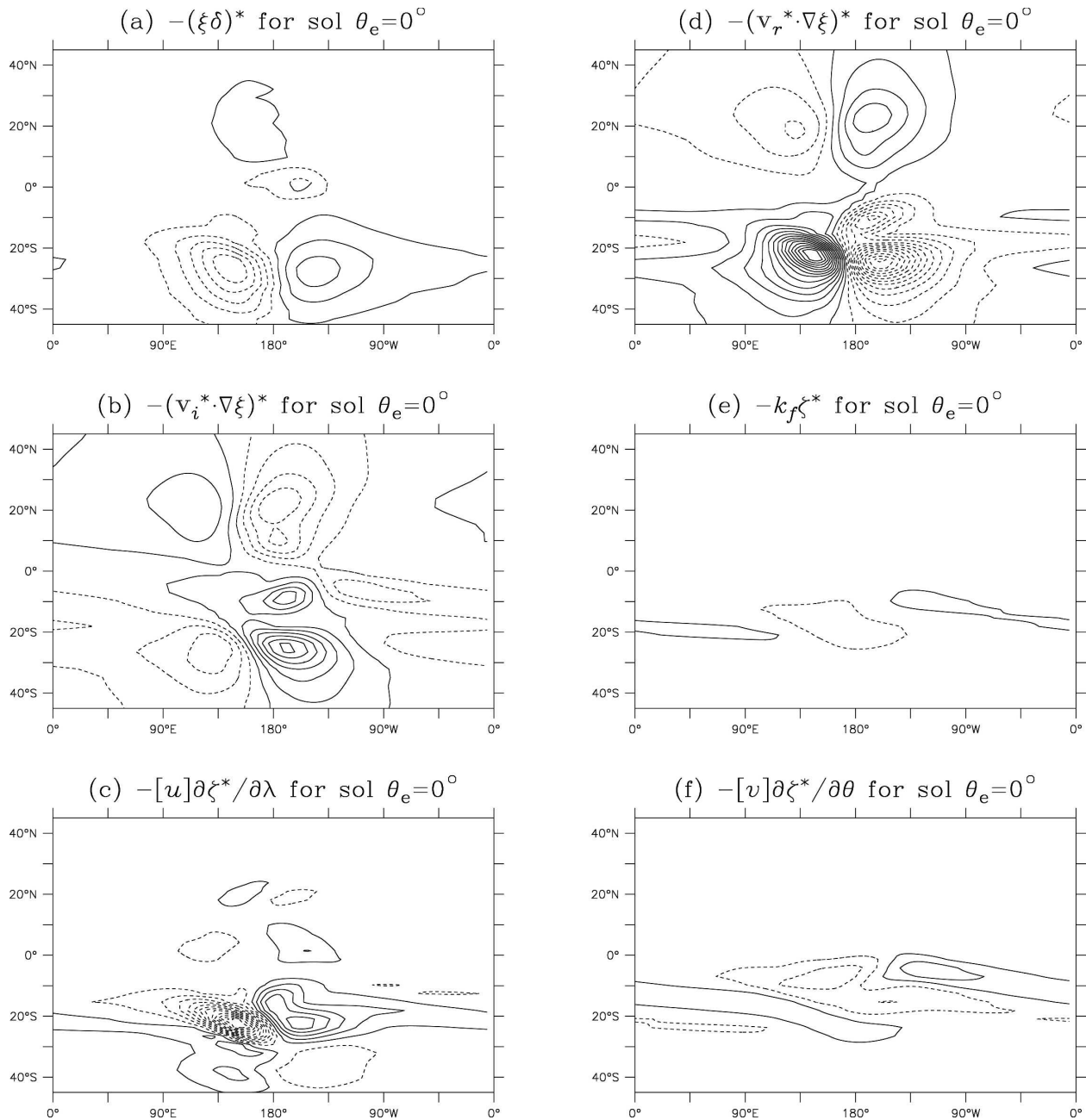


FIG. 8. As in Fig. 6 except for the solstitial $\theta_e = 0^\circ$ experiment.

arises when either the basic state or eddy forcing is asymmetric about the equator. When the eddy forcing and the basic state are both centered at the equator (solid curve in Fig. 10a), which corresponds to equinoctial or annual-mean conditions on earth, the eddy momentum flux is equal and opposite in the two hemispheres, reaching a relatively weak maximum at $\sim 5^\circ$ latitude. When the peak of the zonal-mean topography is moved into the Northern Hemisphere (solid curve in Fig. 10b), the northward flux almost doubles in ampli-

tude, while the southward flux decreases dramatically. Moving the eddy forcing north of the equator in the equinoctial basic state (dashed curve in Fig. 10a) leads to similar but slightly smaller changes in the amplitudes of the northward and southward fluxes, and the pattern also shifts northward by $\sim 8^\circ$. Hence, the eddy momentum fluxes converge in the latitude band where the eddy forcing is located, which is consistent with the general theory of wave propagation through rotating geophysical fluids (Held 1975).

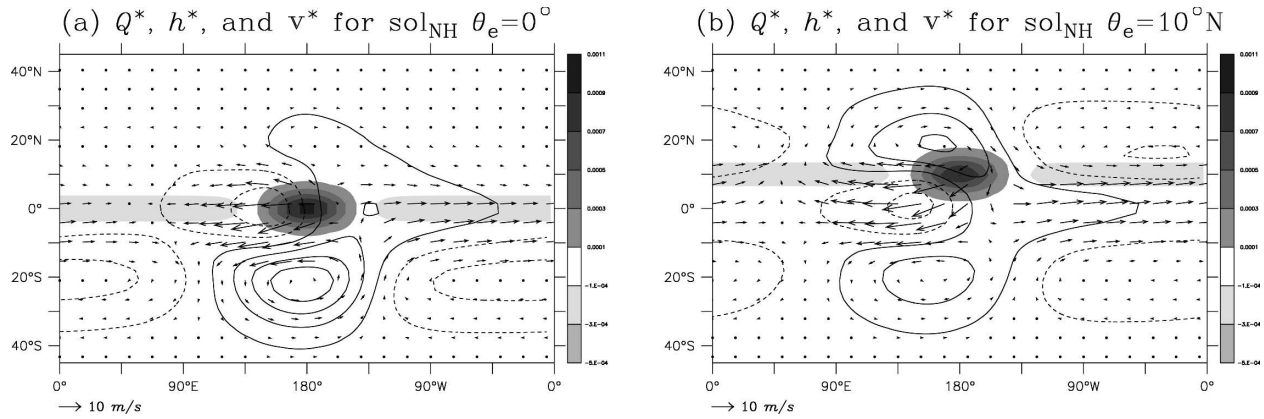


FIG. 9. As in Fig. 5 except for the solstitial no-Hadley basic state.

The eddy momentum fluxes in the solstitial $\theta_e = 10^\circ\text{N}$ model integration (dashed curve in Fig. 10b) are much stronger than those in any other experiment. This agrees with the observed pattern of eddy momentum fluxes in the tropical upper troposphere (Dima et al. 2005), which are strongest during solstitial seasons. The dashed curve in Fig. 10b also closely mirrors, with a change in sign, the mean meridional circulation in the solstitial basic state (Fig. 1e). When the mean meridional flow is removed from the solstitial $\theta_e = 10^\circ\text{N}$ experiment (dotted curve in Fig. 10b), the eddy momentum fluxes decrease dramatically. The eddy momentum fluxes in the other no-Hadley experiments are similar to those in the full basic states. Hence, the anticorrelation between the eddy momentum fluxes and mean meridional winds over the equator in the tropical band can be attributed to the tendency of off-equatorial heating to induce cross-equatorial eddy momentum fluxes and the influence of the mean meridional circulation on the stationary wave response. Experiments with a linearized version of the model (Kraucunas 2005) suggest that nonlinear effects are responsible for about a third of the amplification of the steady eddy momentum fluxes in the solstitial $\theta_e = 10^\circ\text{N}$ experiment.

The amplification of the eddy momentum fluxes near the equator by strong mean meridional flows can also be reproduced in an even simpler model. Consider the steady-state barotropic vorticity equation on an equatorial beta plane, linearized about horizontally uniform zonal and meridional winds U and V , and forced with a fixed vorticity source F :

$$U \frac{\partial \zeta^*}{\partial x} + V \frac{\partial \zeta^*}{\partial y} + \beta_0 v^* = F - k \zeta^*. \quad (14)$$

Here β_0 is the planetary vorticity gradient at the equator, k is the linear damping strength, and x and y represent distance in the zonal and meridional directions,

respectively. To further simplify the problem, consider forcing F and plane wave solutions of the form $\psi^* = Ae^{i(mx+iny)}$ with a single positive zonal wavenumber $m = 2\pi M/a$ (where M is an integer) and a single me-

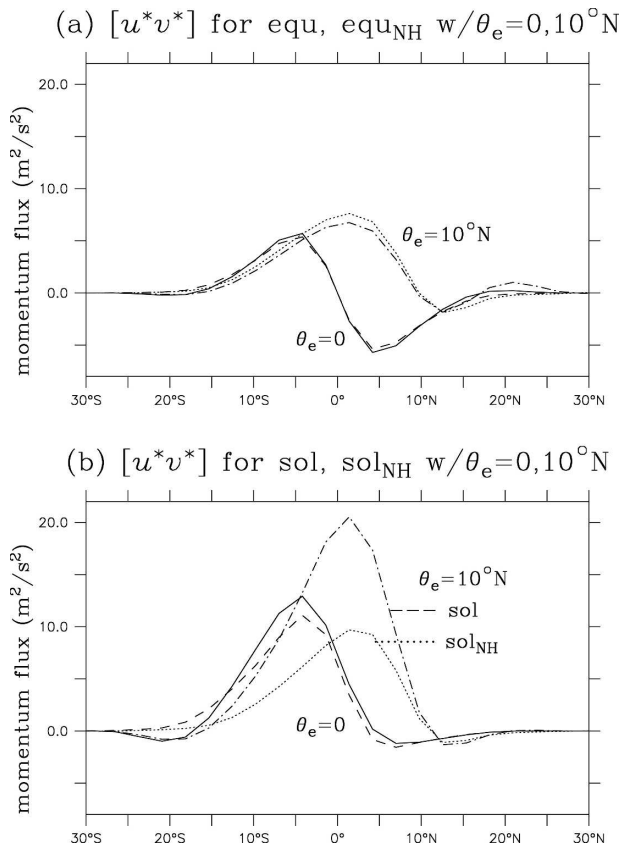


FIG. 10. Eddy momentum fluxes in the (a) equinoctial $\theta_e = 0^\circ$ (solid), equinoctial no-Hadley $\theta_e = 0^\circ$ (dashed), equinoctial $\theta_e = 10^\circ\text{N}$ (dot-dashed), and equinoctial no-Hadley $\theta_e = 10^\circ\text{N}$ (dotted) runs and in the (b) solstitial $\theta_e = 0^\circ$ (solid), solstitial no-Hadley $\theta_e = 0^\circ$ (dashed), solstitial $\theta_e = 10^\circ\text{N}$ (dot-dashed), and solstitial no-Hadley $\theta_e = 10^\circ\text{N}$ (dotted) runs.

ridional wavenumber $n = 2\pi/\alpha_y$ (where α_y is the wavelength) that can be either positive or negative, corresponding to northward and southward moving waves, respectively. Substituting $u^* = -\partial\psi^*/\partial y = -im\psi^*$, $v^* = \partial\psi^*/\partial x = im\psi^*$, and $\xi^* = \nabla^2\psi^* = -(m^2 + n^2)\psi^*$ into (14) yields

$$\psi^* = F[im\beta - (imU - inV + k)(m^2 + n^2)]. \quad (15)$$

Since the forced waves and basic state are identical at all latitudes, the zonally averaged eddy momentum flux is identical to the globally averaged eddy momentum flux and is equal to

$$\begin{aligned} [u^*v^*] &= -mn|\psi^*\psi^{*\dagger}| \\ &= \frac{-mnF^2}{\{m\beta - (m^2 + n^2)(mU + nV)\}^2 + \{k(m^2 + n^2)\}^2}. \end{aligned} \quad (16)$$

Since m is always positive, (16) exhibits the familiar property that waves with positive n (i.e., northward moving waves) are associated with negative (southward) fluxes of momentum, and vice versa. Also note that, when V is zero, the flux for positive n will be equal and opposite to the flux for negative n (i.e., the fluxes associated with northward- and southward-moving waves will be equal and opposite). It is also clear that the magnitude of the momentum flux will increase with the zonal wind speed U . The relationship between V and $[u^*v^*]$ is not immediately obvious, although group velocity considerations (e.g., Watterson and Schneider 1987) might lead one to anticipate that the flux will be enhanced when the wave is traveling in the same direction as the mean meridional flow.

Figure 11 shows the value of $[u^*v^*]$ from (16) over a range of mean meridional wind speeds with $F = 1.5 \times 10^{-11} \text{ s}^{-2}$, $U = -5 \text{ m s}^{-1}$, $k = (10 \text{ days})^{-1}$, $\alpha_y = 45^\circ$, and $M = 1$. These values have been chosen to correspond with the equilibrium steady eddy circulations in the shallow-water experiments, but similar results are obtained over a wide range of parameters. When the mean meridional flow is zero, the positive (northward) eddy momentum fluxes associated with the southward-moving wave ($n < 0$, dashed line) are equal and opposite to the negative (southward) eddy momentum fluxes associated with the northward-moving wave ($n > 0$, solid line), as expected. However, the relative amplitude of the northward and southward momentum fluxes changes dramatically when the mean meridional flow is nonzero, with northward V inducing a large increase in the southward flux and a small decrease in the northward flux, and southward V inducing changes of the opposite sign. Hence, the total eddy momentum

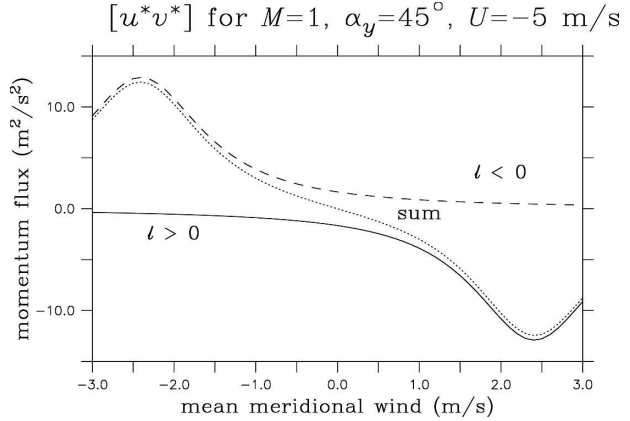


FIG. 11. Eddy momentum fluxes calculated using the linear barotropic model (18) with a mean zonal wind speed of -5 m s^{-1} and eddy forcing at zonal wavenumber-one with a meridional scale of 45° , plotted as a function of mean meridional wind speed.

flux (dotted line) is amplified by, and directed opposite, the mean meridional flow.

5. Conclusions

A nonlinear shallow-water model has been used to explore the influence of hemispheric asymmetry and Earth-like zonal-mean winds on the response to tropical eddy forcing. A novel technique is used to impose realistic basic states in the shallow-water system: a large, zonally symmetric topography distribution that approximates the observed upper-tropospheric geopotential slope is imposed underneath a thin fluid layer. This configuration yields realistic basic-state zonal winds without artificially enhancing tropical wave speeds or neglecting nonlinear terms, thus providing a consistent and versatile framework for studying the influence of different basic states on the steady eddy circulations at low latitudes. A Hadley circulation can be imposed by relaxing the fluid layer toward its initial, global-mean value, or neglected by considering perturbations to a balanced basic state. Both hemispherically symmetric and hemispherically asymmetric basic states are considered. Eddy forcing is imposed by introducing a mass source at, or near, the equator, with a compensating mass sink at other longitudes.

One of the most interesting results of these experiments is that the subtropical eddy height and circulation anomalies exhibit similar amplitudes and horizontal patterns in both hemispheres when the eddy forcing and zonal-mean divergence are both on the equator or both in the same hemisphere. This result suggests that the surprising hemispheric symmetry observed in the seasonally varying tropical stationary waves in the NCEP-NCAR reanalysis (Dima et al. 2005) arises be-

cause the maximum eddy and zonal-mean diabatic heating tend to occur in the same latitude band over the course of the seasonal cycle (see, e.g., Wang and Ting 1999). It is also notable that the amplitude of the stationary wave response is much larger when the eddy forcing and zonal-mean divergence are both located on the same side of the equator than when they are both hemispherically symmetric, in agreement with the observed seasonal cycle in stationary wave amplitudes.

The strength and symmetry of the response to off-equatorial eddy forcing in the solstitial basic state can be explained as follows. The amplification of the eddy response in the summer hemisphere arises because the eddy mass source, and hence the eddy divergence anomaly, is located in a region with a larger zonal-mean total vorticity, which enhances the generation of vorticity by vortex stretching. The amplification of the winter hemisphere response, on the other hand, can be attributed to 1) the advection of vorticity by the eddy divergent wind field, which forces rotational flow across a much broader latitudinal range than the eddy divergence anomaly itself; 2) the stronger zonal-mean zonal winds in the winter hemisphere, which promote a stronger Rossby wave response; and 3) the cross-equatorial mean meridional flow, which enhances the propagation of wave activity in the direction of the flow, as discussed by Watterson and Schneider (1987).

The relatively weak stationary wave response obtained when both the eddy forcing and the basic state are hemispherically symmetric, on the other hand, can be attributed to the large anticyclonic vorticity anomalies that form on either side of the equator, which reduce the vorticity and vorticity gradient in the vicinity of the mass source. Were it not for the advection of vorticity by the eddy divergent winds, which operate over a much broader latitudinal scale than the vortex stretching associated with the eddy divergence anomaly, the response to eddy forcing centered on the equator would be very small. Sardesmukh and Hoskins (1988) reached a similar conclusion regarding the global stationary wave response to a fixed tropical eddy divergence anomaly in a barotropic model.

The seasonal variations in the low-latitude eddy momentum fluxes reported by Dima et al. (2005) can also be attributed to the tendency for the maximum zonal-mean and eddy forcing to occur in the same latitude band. Hemispheric asymmetry in either the mean meridional flow or tropical eddy forcing produces steady eddy momentum fluxes that are directed across the equator. The momentum flux is strongest near the equator because the flow is less constrained by planetary rotation and because the weak horizontal vorticity gradients near the equator allow stronger eddy me-

ridional winds. The momentum fluxes are enhanced when the eddy forcing and zonal-mean divergence are located in the same hemisphere because the eddy response is strong in both hemispheres, and because cross-equatorial mean meridional flow enhances the propagation of wave activity across the equator. Hence, the eddy momentum fluxes associated with the tropical stationary wave response are anticorrelated with the mean meridional flow and strongest when the basic state and eddy forcing are both hemispherically asymmetric, which mirrors the relationship between the observed seasonally varying large-scale waves and mean meridional flow in the equatorial upper troposphere.

Another important conclusion arising from the shallow-water model experiments described here is that the presence of westerly zonal-mean winds in the subtropics shifts the centers of subtropical vorticity and height anomalies eastward relative to their positions in a resting basic state. Divergence and convergence anomalies induced by the strong rotational flow on either side of the mass source also play an important role in controlling the size and shape of the eddy response in realistic basic states; this feedback would not be resolved in a barotropic model or a model with fixed eddy divergence anomalies. All of these features are reproduced in a linearized version of the model (Kraucunas 2005). This makes it unlikely that nonlinearity is responsible for the eastward displacement of the subtropical anticyclones, as suggested by Hendon (1986). However, the centers of rotational flow are still centered slightly to the west of the mass source in all of the shallow-water experiments, whereas the observed subtropical anticyclones are usually centered directly poleward of the strongest eddy forcing. The results of Ting and Held (1990) suggest that transient eddy fluxes could be responsible for this remaining discrepancy, although the moderately strong drag used in our model might also be a factor. Both the position of the subtropical anticyclones and the hemispheric symmetry of the response to tropical eddy forcing could also be influenced by the presence of zonal asymmetry in the basic state, a possibility that could be explored in future work.

Acknowledgments. This research was inspired by a series of experiments performed by Jim Holton in late 2003, and also benefited from conversations with Mike Wallace, Ioana Dima, and Dave Lorenz. The authors would also like to thank two anonymous reviewers for their comments. This work was supported by NSF Grant ATM-0409075.

REFERENCES

- Brunet, G., and P. H. Haynes, 1996: Low-latitude reflection of Rossby wave trains. *J. Atmos. Sci.*, **53**, 482–496.

- Dima, I., J. M. Wallace, and I. Kraucunas, 2005: Tropical angular momentum balance in the NCEP reanalysis. *J. Atmos. Sci.*, **62**, 2499–2513.
- Esler, J. G., L. M. Polvani, and R. A. Plumb, 2000: The effect of a Hadley circulation on the propagation and reflection of planetary waves in a simple one-level model. *J. Atmos. Sci.*, **57**, 1536–1556.
- Gent, P. R., 1993: The energetically consistent shallow-water equations. *J. Atmos. Sci.*, **50**, 1323–1325.
- Gill, A. E., 1980: Some simple solutions for heat-induced tropical circulation. *Quart. J. Roy. Meteor. Soc.*, **106**, 447–462.
- , 1980: *Atmosphere–Ocean Dynamics*. International Geophysics Series, Vol. 30, Academic Press, 662 pp.
- , and P. J. Phillips, 1986: Nonlinear effects on the heat-induced circulations of the tropical atmosphere. *Quart. J. Roy. Meteor. Soc.*, **112**, 69–91.
- Held, I. M., 1975: Momentum transport by quasi-geostrophic eddies. *J. Atmos. Sci.*, **33**, 1494–1497.
- , and A. Y. Hou, 1980: Nonlinear axially symmetric circulations in a nearly inviscid atmosphere. *J. Atmos. Sci.*, **37**, 515–533.
- , and P. J. Phillips, 1990: A barotropic model of the interaction between the Hadley cell and a Rossby wave. *J. Atmos. Sci.*, **47**, 856–869.
- Hendon, H. H., 1986: The time-mean flow and variability in a nonlinear model of the atmosphere with tropical diabatic forcing. *J. Atmos. Sci.*, **43**, 72–88.
- Hoskins, B. J., and M. J. Rodwell, 1995: A model of the Asian summer monsoon. Part I: The global scale. *J. Atmos. Sci.*, **52**, 1329–1340.
- , R. Neale, M. Rodwell, and G.-Y. Yang, 1999: Aspects of the large-scale tropical atmospheric circulation. *Tellus*, **51**, 33–44.
- Hsu, C. J., and R. A. Plumb, 2000: Non-axisymmetric thermally driven circulations and upper tropospheric monsoon dynamics. *J. Atmos. Sci.*, **57**, 1254–1276.
- Kraucunas, I., 2005: The influence of hemispheric asymmetry and realistic basic states on tropical stationary waves in a nonlinear shallow water model. Ph.D. dissertation, University of Washington, 99 pp.
- , and D. L. Hartmann, 2005: Equatorial superrotation and the factors controlling the zonal-mean zonal winds in the tropical upper troposphere. *J. Atmos. Sci.*, **62**, 371–389.
- Lau, K.-M., and H. Lim, 1982: Thermally driven motions in an equatorial β -plane: Hadley and Walker circulations during the winter monsoon. *Mon. Wea. Rev.*, **110**, 336–353.
- , and —, 1984: On the dynamics of equatorial forcing of climate teleconnections. *J. Atmos. Sci.*, **41**, 161–176.
- Lim, H., and C.-P. Chang, 1983: Dynamics of teleconnections and Walker circulations forced by equatorial heating. *J. Atmos. Sci.*, **40**, 1897–1915.
- Lindzen, R. S., and A. Y. Hou, 1988: Hadley circulations for zonally averaged heating centered off the equator. *J. Atmos. Sci.*, **45**, 2416–2427.
- Matsuno, T., 1966: Quasi-geostrophic motions in the equatorial area. *J. Meteor. Soc. Japan*, **44**, 25–42.
- Nieto Ferreira, R., and W. H. Schubert, 1999: The role of tropical cyclones in the formation of tropical upper-troposphere troughs. *J. Atmos. Sci.*, **56**, 2891–2907.
- Philips, P. J., and A. E. Gill, 1987: An analytic model of the heat-induced tropical circulation in the presence of a mean wind. *Quart. J. Roy. Meteor. Soc.*, **113**, 213–236.
- Sardeshmukh, P. D., and B. J. Hoskins, 1985: Vorticity balances in the tropics during the 1982–1983 El Niño–Southern Oscillation event. *Quart. J. Roy. Meteor. Soc.*, **111**, 261–278.
- , and —, 1988: The generation of global rotational flow by steady idealized tropical divergence. *J. Atmos. Sci.*, **45**, 1228–1251.
- Schneider, E. K., and I. G. Watterson, 1984: Stationary Rossby wave propagation through easterly layers. *J. Atmos. Sci.*, **41**, 2069–2083.
- Schumacher, C., R. A. Houze Jr., and I. Kraucunas, 2004: The tropical dynamical response to latent heating estimates derived from the TRMM precipitation radar. *J. Atmos. Sci.*, **61**, 1341–1358.
- Ting, M., and I. M. Held, 1990: The stationary wave response to a tropical SST anomaly in an idealized GCM. *J. Atmos. Sci.*, **47**, 2546–2566.
- , H. Wang, and L. Yu, 2001: Nonlinear stationary wave maintenance and seasonal cycle in the GFDL R30 GCM. *J. Atmos. Sci.*, **58**, 2331–2354.
- Van Tuyl, A. H., 1986: Advective influences on forced tropical motions. *J. Atmos. Sci.*, **43**, 141–161.
- Wang, H., and M. Ting, 1999: Seasonal cycle of the climatological stationary waves in the NCEP–NCAR reanalysis. *J. Atmos. Sci.*, **56**, 3892–3919.
- Watterson, I. G., and E. K. Schneider, 1987: The effect of the Hadley circulation on the meridional propagation of stationary waves. *Quart. J. Roy. Meteor. Soc.*, **113**, 779–813.
- Webster, P. J., and H.-R. Chang, 1988: Energy accumulation and emanation regions at low latitudes: Impacts of a zonally varying basic state. *J. Atmos. Sci.*, **45**, 803–829.
- Wheeler, M., G. N. Kiladis, and P. J. Webster, 2000: Large-scale dynamical fields associated with convectively coupled equatorial waves. *J. Atmos. Sci.*, **57**, 613–640.